DALTON
FULL PAPER

Activation of H_2 by halogenocarbonylbis(phosphine)rhodium(I) complexes. The use of parahydrogen induced polarisation to detect species present at low concentration

Paul D. Morran,[a] Simon B. Duckett,*[a] Peter R. Howe,[a] John E. McGrady,[a] Simon A. Colebrooke,[a] Richard Eisenberg,*[b] Martin G. Partridge[a] and Joost A. B. Lohman[c]

[a] *Department of Chemistry, University of York, Heslington, York, UK YO10 5DD*
[b] *Department of Chemistry, University of Rochester, Rochester, NY 14627, USA*
[c] *Bruker UK Limited, Coventry, UK*

Received 25th June 1999, Accepted 5th October 1999

Complexes of the form $RhX(CO)(PR_3)_2$ [X = Cl, Br or I; R = Me or Ph] reacted with H_2 to form a series of binuclear complexes of the type $(PR_3)_2H_2Rh(\mu\text{-}X)_2Rh(CO)(PR_3)$ [X = Cl, Br or I, R = Ph; X = I, R = Me] and $(PMe_3)_2(X)HRh(\mu\text{-}H)(\mu\text{-}X)Rh(CO)(PMe_3)$ [X = Cl, Br or I] according to parahydrogen sensitised ^1H, ^{13}C, ^{31}P and ^{103}Rh NMR spectroscopy. Analogous complexes containing mixed halide bridges $(PPh_3)_2H_2Rh(\mu\text{-}X)(\mu\text{-}Y)Rh(CO)(PPh_3)$ [X, Y = Cl, Br or I; X ≠ Y] are detected when $RhX(CO)(PPh_3)_2$ and $RhY(CO)(PPh_3)_2$ are warmed together with p-H_2. In these reactions only one isomer of the products $(PPh_3)_2H_2Rh(\mu\text{-}I)(\mu\text{-}Cl)Rh(CO)(PPh_3)$ and $(PPh_3)_2H_2Rh(\mu\text{-}I)(\mu\text{-}Br)Rh(CO)(PPh_3)$ is formed in which the μ-iodide is *trans* to the CO ligand of the rhodium(I) centre. When $(PPh_3)_2H_2Rh(\mu\text{-}Cl)(\mu\text{-}Br)Rh(CO)(PPh_3)$ is produced in the same way two isomers are observed. The mechanism of the hydrogen addition reaction is complex and involves initial formation of $RhH_2X(CO)(PR_3)_2$ [R = Ph or Me], followed by CO loss to yield $RhH_2X(PR_3)_2$. This intermediate is then attacked by the halide of a precursor complex to form a binuclear species which yields the final product after PR_3 loss. The $(PPh_3)_2H_2Rh(\mu\text{-}X)_2Rh(CO)(PPh_3)$ systems are shown to undergo hydride self exchange by exchange spectroscopy with rates of 13.7 s^{-1} for the $(\mu\text{-}Cl)_2$ complex and 2.5 s^{-1} for the $(\mu\text{-}I)_2$ complex at 313 K. Activation parameters indicate that ordering dominates up to the rate determining step; for the $(\mu\text{-}Cl)_2$ system $\Delta H^{\ddagger} = 52 \pm 9$ kJ mol^{-1} and $\Delta S^{\ddagger} = -61 \pm 27$ J K^{-1} mol^{-1}. This process most likely proceeds *via* halide bridge opening at the rhodium(III) centre, rotation of the rhodium(III) fragment around the remaining halide bond and bridge re-establishment. If the triphenylphosphine ligands are replaced by trimethylphosphine distinctly different reactivity is observed. When $RhX(CO)(PMe_3)_2$ [X = Cl or Br] is warmed with p-H_2 the complex $(PMe_3)_2(X)HRh(\mu\text{-}H)(\mu\text{-}X)Rh(CO)(PMe_3)$ [X = Cl or Br] is detected which contains a bridging hydride *trans* to the rhodium(I) PMe_3 ligand. However, when X = I, the situation is far more complex, with $(PMe_3)_2H_2Rh(\mu\text{-}I)_2Rh(CO)(PMe_3)$ observed preferentially at low temperatures and $(PMe_3)_2(I)HRh(\mu\text{-}H)(\mu\text{-}I)Rh(CO)(PMe_3)$ at higher temperatures. Additional binuclear products corresponding to a second isomer of $(PMe_3)_2(I)HRh(\mu\text{-}H)(\mu\text{-}I)Rh(CO)(PMe_3)$, in which the bridging hydride is *trans* to the rhodium(I) CO ligand, and $(PMe_3)_2HRh(\mu\text{-}H)(\mu\text{-}I)_2Rh(CO)(PMe_3)$ are also observed in this reaction. The relative stabilities of related systems containing the phosphine PH_3 have been calculated using approximate density functional theory. In each case, the $(\mu\text{-}X)_2$ complex is found to be the most stable, followed by the $(\mu\text{-}H)(\mu\text{-}X)$ species with hydride *trans* to PH_3.

Introduction

The observation and characterisation of species present in low concentrations during a reaction is the key to developing a full understanding of the system under study. During the past decade, parahydrogen induced polarisation (PHIP) has been used for reactions involving H_2 to provide just this information.[1] In parahydrogen induced polarisation,[2] originally formulated by Bowers and Weitekamp[3] as the PASADENA effect, enhanced absorption and emission signals occur in product NMR spectra if dihydrogen enriched in the para spin state is added pairwise to a metal centre or organic substrate while maintaining spin correlation between the transferred protons.[4] Specifically, parahydrogen with its αβ-βα nuclear spin state populates αβ and βα levels (relative to αα and ββ) of the product H_aH_b spin system so that both protons, H_a and H_b, exhibit enhanced antiphase resonances. Theoretically, the magnitude of enhancement can be as large as 28,500 and, in practice, enhancements of around a thousandfold have been seen.[5]

The non-Boltzmann population of the H_aH_b spin system generated with PHIP can also result in enhancement of scalar coupled ^{31}P and ^{13}C heteronuclei by cross-relaxation[6] or in conjunction with polarisation transfer sequences such as INEPT+ (insensitive nuclei enhanced by polarisation transfer).[7] For the latter, signal-to-noise ratio increases of up to 25,000 have been achieved. More recently, the SEPP (*s*elective *e*xcitation of *p*olarisation using *P*ASADENA) sequence has been developed by Bargon and co-workers[8,9] to remove the need for π/4 pulse excitation with parahydrogen. Furthermore, because the occurrence of ^{13}C–^{13}C groupings is 100 times lower than the basic ^{13}C level, experiments designed to monitor this arrangement are extremely insensitive and typically take many hours to complete. Natterer *et al.*[10] have completed this sort of measurement with p-H_2 in minutes when examining alkyne hydrogenation products. Parahydrogen induced polarisation has also been used in conjunction with 2-D methods such as heteronuclear multiple quantum coherence spectroscopy (HMQC), to facilitate rapid indirect observation of insensitive nuclei such as ^{103}Rh and ^{195}Pt from sub-milligram samples.[11,12]

To date, PHIP has been used to characterise metal dihydrides formed by H_2 oxidative addition to a number of metal complexes including those of Ru^0, Rh^I, Ta^{III}, Ir^I and Pt^0.[13] Complexes of Rh^I are particularly interesting because their

reactions with H_2 are often thermodynamically unfavourable, meaning that product dihydrides, when compared with their iridium counterparts, are relatively unstable or form to only a minor extent. This reduced stability accounts for complexes of Rh^I such as $RhCl(PPh_3)_3$ or Wilkinson's catalyst being effective homogeneous hydrogenation catalysts. For $RhCl(PPh_3)_3$, PHIP has been used to detect minor species under catalytic conditions including the olefin dihydride complex $Rh(H)_2Cl(alkene)(PPh_3)_2$.[14] Hydrogenation of itaconic acid [$HO_2CCH_2C(=CH_2)CO_2H$] by the rhodium catalysts Rh(NBD)(bisphosphinite)BF_4 (bisphosphinite = 2,3-O-bis(diphenylphosphino)-β-D-glucopyranoside) has also been observed to yield p-H_2 enhanced hydride resonances for a potential intermediate in the hydrogenation cycle.[15]

Here we describe how parahydrogen induced polarisation allows the mapping of previously unseen reactions and therefore enables the complexity of a hydrogen reaction system to be appreciated fully. The studies described in this paper analyse the reactivity of the rhodium(I) complexes $RhX(CO)(PR_3)_2$ **1** where X = Cl, Br or I and R = Ph or Me. A numbering scheme which identifies the complex type, the halide and the phosphine such that $RhCl(CO)(PPh_3)_2$ is **1-[Cl-Ph]** has been followed throughout.

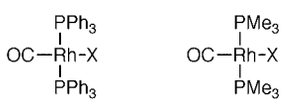

1-[X-Ph] 1-[X-Me]

X = Cl, Br or I

Chart 1

The parent member of this series, **1-[Cl-Ph]**, was first synthesized in 1957 and is one of the best known complexes of rhodium(I).[16] This complex is readily formed from $RhCl(PPh_3)_3$ by CO addition or aldehyde decarbonylation,[17] undergoes facile photodissociation of CO and functions as a photo-catalyst for benzene carbonylation.[18,19] However, in contrast to its iridium(I) analogue, Vaska's complex, which oxidatively adds H_2 readily with an equilibrium constant of $>10^3$,[20] $RhCl(CO)(PPh_3)_2$ had not previously been seen to react with dihydrogen directly. Through the use of parahydrogen induced polarisation, however, limited reaction was found to occur and a new dihydride species containing both Rh(III) and Rh(I) centres was detected.[21] The corresponding PMe_3 complex was also observed to react, yielding a related dihydride product. In this paper we expand on those earlier communications and present a full study of H_2 addition to $RhX(CO)(PR_3)_2$ (X = Cl, Br or I; R = Ph or Me). The study, based on PHIP, reveals many new dihydride products, examines their dynamic behaviour and gives an analysis of the mechanism of their formation. The bonding in binuclear systems has been studied in a theoretical context by a number of authors,[22] but previous studies on rhodium-based catalysis have focused exclusively on mononuclear species.[23] We also use approximate density functional theory[24] to analyse the relative stabilities of the various binuclear products identified using PHIP.

Experimental

All sample preparations were completed using either a nitrogen filled glove box or a Schlenk line. Solvents were dried over potassium and degassed prior to use. The NMR measurements were made using NMR tubes fitted with J. Young Teflon valves and solvents added by vacuum transfer on a high vacuum line. Triphenylphosphine (Aldrich), trimethylphosphine (Aldrich) and hydrogen (99.99%, BOC) were used as received. The complexes $RhCl(CO)(PPh_3)_2$, **1-[Cl-Ph]**, and $RhCl(CO)(PMe_3)_2$, **1-[Cl-Me]**, were prepared according to established methods and then used respectively in the synthesis of $RhBr(CO)(PPh_3)_2$, **1-[Br-Ph]**, and $RhI(CO)(PPh_3)_2$, **1-[I-Ph]**, and $RhBr(CO)(PMe_3)_2$, **1-[Br-Me]**, and $RhI(CO)(PMe_3)_2$, **1-[I-Me]**.[16]

For the PHIP experiments, hydrogen enriched in the para spin state was prepared by cooling H_2 to 77 K over a paramagnetic catalyst as described previously.[14] An atmosphere of H_2 equivalent to *ca.* 3 atm pressure at 298 K was introduced into a resealable NMR tube on a high vacuum line. The samples were thawed immediately prior to use and introduced into the NMR spectrometer at the pre-set temperature. Parahydrogen-enhanced NMR spectra were recorded on Bruker AMX-500 and DRX-400 spectrometers with ^1H at 500.13 and 400.13, ^{31}P at 253 and 161.9, ^{13}C at 125.1 and 100, and ^{103}Rh at 15.737 MHz, respectively. The ^1H NMR chemical shifts are reported in ppm relative to residual ^1H signals in the deuteriated solvents (benzene-d_5, δ 7.13, and toluene-d_7, δ 2.13), $^{31}P\{^1H\}$ NMR in ppm downfield of an external 85% solution of phosphoric acid, ^{13}C NMR relative to benzene-d_6, δ 128.0, and toluene-d_8, δ 21.3, and ^{103}Rh relative to 15.80 MHz, δ 0. Modified ^1H–^1H -COSY, -HMQC, and -NOESY pulse sequences were used as previously described.[12]

The NOE spectra were analysed according to standard methods.[25] Importantly, no exchange cross peaks to free hydrogen were observed for the range of mixing times used to extract rate information and a simple two-site exchange mechanism was assumed. The rate of hydride interchange, k/s^{-1}, was determined for a mixing time, t_m, using eqn. (1) where I is the ratio of intensities of the diagonal and exchange cross peaks.

$$k = \frac{1}{t_m}\ln\left(\frac{I+1}{I-1}\right) \quad (1)$$

All calculations described in this paper are based on approximate density functional theory, which has been used with great success to probe structure, energetics and mechanisms in transition metal-based systems.[26] Calculations were performed using the Amsterdam Density Functional (ADF) program Version 2.3, developed by Baerends and co-workers.[27] A double-ζ Slater basis set extended with a single p (H) or d (C, N, O, P, Cl, Br) polarisation function was used to describe the main group atoms, while a triple-ζ basis was used for Rh + I. Electrons in orbitals up to and including 1s {C,O}, 2p{P, Cl}, 3p{Cr}, 3d{Br}, 4p{Rh} and 4d {I} were considered to be part of the core and treated in accordance with the frozen core approximation. The local density approximation was employed in all cases,[24] along with the local exchange-correlation potential of Vosko, *et al.*[28] and gradient corrections to exchange (Becke)[29] and correlation (Perdew).[30] All structures were optimised using the gradient algorithm of Versluis and Ziegler.[31] In the model complexes, the aryl and alkyl groups of PPh_3 and PMe_3 respectively are replaced by hydrogen atoms.

Results and discussion

Reactions of $RhX(CO)(PPh_3)_2$ [X = Cl, Br or I] with hydrogen

When a 1mM solution of $RhCl(CO)(PPh_3)_2$, **1-[Cl-Ph]**, in benzene-d_6 is warmed with *ca.* 3 atm p-H_2 and monitored by ^1H NMR spectroscopy two sets of hydride resonances are detected at δ −19.31 and −19.66. These resonances, illustrated in Fig. 1a, are assigned to the hydride ligands H_a and H_b respectively of the binuclear product **2-[Cl-Cl-Ph]** shown in Chart 2 (the dinuclear complexes are labelled [X-Y-Z] where X is the bridging ligand *trans* to CO, Y *trans* to phosphine, and Z the substituent on the PZ_3 ligand). Initially, these signals are only observed at temperatures above 343 K, but on degassing and refilling the sample with p-H_2 they become observable at temperatures as low as 318 K. Each of these hydride resonances appears as a quartet of antiphase doublets with their

anti-phase character confirming that these protons originate from parahydrogen. The corresponding ^{1}H-{^{31}P} spectrum (Fig. 1b) simplifies the original spectrum to the extent that the two hydride resonances now appear as doublets of antiphase doublets with J_{RhHa} = 24.7, J_{RhHb} = 24.6 Hz and J_{HH} = −11 Hz. A gradient assisted ^{1}H–^{31}P heteronuclear multiple quantum correlation (HMQC) experiment was used to probe the ^{31}P nuclei in this product. In this NMR experiment the parahydrogen derived magnetisation is first transferred to phosphorus where it precesses under the influence of the phosphorus chemical shift before it is returned to the proton domain for detection. This indirect approach makes optimum use of the proton enhancement to obtain heteronuclear chemical shift data. The P–H couplings are removed in the ^{1}H domain by decoupling during acquisition and in the ^{31}P domain by applying a 180° refocusing pulse to ^{1}H during ^{31}P chemical shift evolution. The resulting 2-D map therefore contains two rhodium coupled hydride resonances that are connected to a single type of ^{31}P nucleus which resonates at δ 40.0 and is coupled to rhodium with J_{RhP} = 118 Hz (Fig. 1c). In view of the fact that the reported values of $^1J_{Rh(III)P}$ and $^1J_{Rh(I)P}$ for {P(C$_6$H$_4$Me-*p*)$_3$}H$_2$Rh(μ-Cl)$_2$Rh{P(C$_6$H$_4$Me-*p*)$_3$}$_2$ are 116 and 193 Hz, and for [Rh(μ-Cl){P(C$_6$H$_4$Me-*p*)$_3$}$_2$]$_2$ are 195 Hz respectively, the size of this coupling indicates that the ^{31}P nucleus is connected to a rhodium(III) centre.[32] A 2-D ^{1}H–^{103}Rh HMQC experiment was used to observe the ^{103}Rh nucleus; this was possible even though ^{103}Rh is 32,000 times less sensitive to direct observation than ^{1}H. In this experiment both of the hydride resonances were observed to connect to a rhodium(III) centre that resonates at δ 925 and is coupled to two ^{31}P nuclei (Fig. 1d).

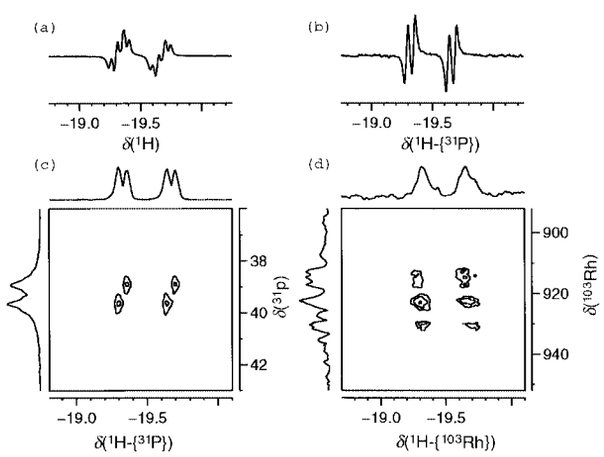

Fig. 1 The NMR spectra of the product **2-[Cl-Cl-Ph]**, formed by warming RhCl(CO)(PPh$_3$)$_2$, **1-[Cl-Ph]**, with p-H$_2$ in C$_6$D$_6$ at 348 K: (a) ^{1}H spectrum showing the two hydride resonances; (b) ^{1}H-{^{31}P} spectrum; (c) selected cross peaks (absolute value display) and projections in the ^{1}H–^{31}P HMQC correlation spectrum (^{31}P decoupled); (d) selected cross peaks (absolute value display) and projections in the ^{1}H–^{103}Rh HMQC correlation spectrum.

The data summarised above establish that the product contains a Rh^{III}H$_2$(PPh$_3$)$_2$ core. Additionally, because the hydride resonances of **2-[Cl-Cl-Ph]** have chemical shifts which are close and somewhat upfield, it can be concluded that the chemically inequivalent hydrides are *trans* to similar chloride ligands in the product. Subsequent studies involving other halides, which are detailed below, confirm this conclusion. The presence of only one other ligand, namely carbon monoxide, needed to be established in order to assign the structure of **2-[Cl-Cl-Ph]**. When the H$_2$ addition reaction was performed using ^{13}CO-labelled **1-[Cl-Ph]** no ^{13}C coupling was observed in the product dihydride resonances and the spectra were identical to those obtained from unlabelled complex. However, when the dinuclear complex [Rh(μ-Cl)(PPh$_3$)$_2$]$_2$ was treated with p-H$_2$, polarised resonances were not seen, and instead only a hydride resonance at δ −19.72 originally reported by Tolman *et al.*[32] was observed, indicative of (PPh$_3$)$_2$H$_2$Rh(μ-Cl)$_2$Rh(PPh$_3$)$_2$. In Tolman's system, two equivalent hydrides are bound to a rhodium(III) centre which in turn is connected by chloride bridges to a second Rh centre maintained in the +1 oxidation state. When the same reaction was repeated with p-H$_2$ at 352 K in the presence of 1-butanal a good decarbonylation substrate and hence CO source, enhanced resonances identical to those seen with **1-[Cl-Ph]** and p-H$_2$ were observed. These experiments clearly indicated that CO is an essential component of the reaction that generates **2-[Cl-Cl-Ph]**.

When [Rh(μ-Cl)(PPh$_3$)$_2$]$_2$ and **1-[Cl-Ph]** were warmed together in the presence of hydrogen the hydride resonances corresponding to **2-[Cl-Cl-Ph]** and (PPh$_3$)$_2$H$_2$Rh(μ-Cl)$_2$Rh(PPh$_3$)$_2$ were observed under normal conditions. An additional resonance was observed in the corresponding directly detected ^{31}P-{^{1}H} spectrum that required **2-[Cl-Cl-Ph]** to contain an additional phosphorus ligand (δ 53, J_{RhP} = 196 Hz) which couples to a rhodium(I) centre. Based on the observations outlined above and the structure of Tolman's dihydride complex, we are able to assign the structure of **2-[Cl-Cl-Ph]** as the binuclear complex (PPh$_3$)$_2$H$_2$Rh(μ-Cl)$_2$Rh(CO)(PPh$_3$) with hydrides *trans* to chloride bridges and rendered inequivalent by ligands *trans* to the chlorides on the rhodium(I) centre as indicated below.

When the bromide and iodide analogues of **1-[Cl-Ph]** are warmed with p-H$_2$, the corresponding binuclear products (PPh$_3$)$_2$H$_2$Rh(μ-Br)$_2$Rh(CO)(PPh$_3$), **2-[Br-Br-Ph]**, and (PPh$_3$)$_2$H$_2$Rh(μ-I)$_2$Rh(CO)(PPh$_3$), **2-[I-I-Ph]**, are detected. While the chemical shifts of the two inequivalent hydride resonances of **2-[Br-Br-Ph]** prove to be so similar, δ −18.47 and −18.52, that they are second order even at 500 MHz, those of **2-[I-I-Ph]** at

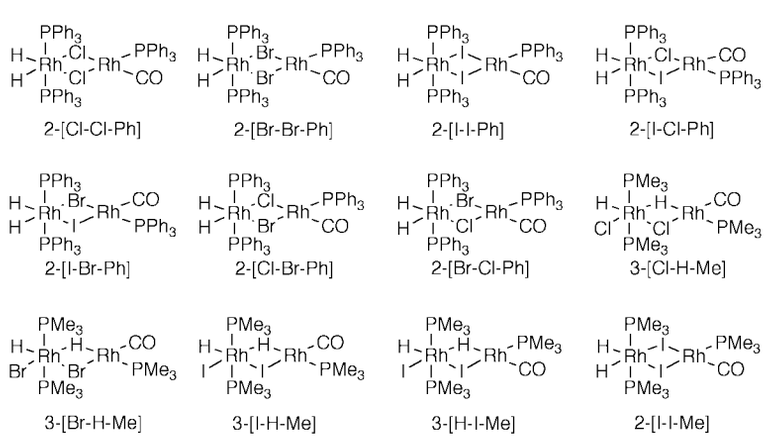

Chart 2

Table 1 ^{1}H NMR Data for complexes **2**–**4**[a]

Complex	Formula	T/K	δ (J/Hz)
2-[Cl-Cl-Ph]	$(PPh_3)_2H_2Rh(\mu\text{-}Cl)_2Rh(CO)(PPh_3)$	318	−19.31 (ddt, $^2J_{HH}$ = −11, $^1J_{RhH}$ = 24.7, $^2J_{PH}$ = 16.3) −19.66 (ddt, $^2J_{HH}$ = −11, $^1J_{RhH}$ = 24.6, $^2J_{PH}$ = 14.5)
2-[Br-Br-Ph]	$(PPh_3)_2H_2Rh(\mu\text{-}Br)_2Rh(CO)(PPh_3)$	323	−18.47 (ddt, $^2J_{HH}$ = −9.5, $^1J_{RhH}$ = 21.0, $^2J_{PH}$ = 11.0) −18.52 (ddt, $^2J_{HH}$ = −9.5, $^1J_{RhH}$ = 21.4, $^2J_{PH}$ = 11.5)
2-[I-I-Ph]	$(PPh_3)_2H_2Rh(\mu\text{-}I)_2Rh(CO)(PPh_3)$	313	−16.35 (ddt, $^2J_{HH}$ = −8.6, $^1J_{RhH}$ = 24.2, $^2J_{PH}$ = 12.0) −16.72 (ddt, $^2J_{HH}$ = −8.6, $^1J_{RhH}$ = 23.5, $^2J_{PH}$ = 13.0)
2-[I-Cl-Ph]	$(PPh_3)_2H_2Rh(\mu\text{-}Cl)(\mu\text{-}I)Rh(CO)(PPh_3)$	318	−16.57 (ddt, $^2J_{HH}$ = −7.8, $^1J_{RhH}$ = 25.5, $^2J_{PH}$ = 11.2) −19.58 (ddt, $^2J_{HH}$ = −7.8, $^1J_{RhH}$ = 23.5, $^2J_{PH}$ = 10.0)
2-[I-Br-Ph]	$(PPh_3)_2H_2Rh(\mu\text{-}Br)(\mu\text{-}I)Rh(CO)(PPh_3)$	323	−16.61 (ddt, $^2J_{HH}$ = −8.0, $^1J_{RhH}$ = 24.8, $^2J_{PH}$ = 13.5) −18.51 (ddt, $^2J_{HH}$ = −8.0, $^1J_{RhH}$ = 24.8, $^2J_{PH}$ = 14.5)
2-Br-Cl-Ph]	$(PPh_3)_2H_2Rh(\mu\text{-}Cl)(\mu\text{-}Br)Rh(CO)(PPh_3)$	323	−18.43 (ddt, $^2J_{HH}$ = −11.1, $^1J_{RhH}$ = 25.5, $^2J_{PH}$ = 14.7) −19.58 (ddt, $^2J_{HH}$ = −11.1, $^1J_{RhH}$ = 21.6, $^2J_{PH}$ = 16.7)
2-[Cl-Br-Ph]	$(PPh_3)_2H_2Rh(\mu\text{-}Cl)(\mu\text{-}Cl)(\mu\text{-}Br)Rh(CO)(PPh_3)$	323	−18.54 (ddt, $^2J_{HH}$ = −11.2, $^1J_{RhH}$ = 24.5, $^2J_{PH}$ = 14.7) −19.33 (ddt, $^2J_{HH}$ = −11.2, $^1J_{RhH}$ = 22.6, $^2J_{PH}$ = 16.7)
2-[I-I-Me]	$(PMe_3)_2H_2Rh(\mu\text{-}I)_2Rh(CO)(PMe_3)$	318	−17.70 (ddt, $^2J_{HH}$ = −9, $^1J_{RhH}$ = 32, $^2J_{PH}$ = 15.6) −18.02 (ddt, $^2J_{HH}$ = −9, $^1J_{RhH}$ = 30.7, $^2J_{PH}$ = 16.3)
3-[Cl-H-Me]	$(PMe_3)_2ClHRh(\mu\text{-}Cl)(\mu\text{-}H)Rh(CO)(PMe_3)$	318	−17.10 (ddddt, $^2J_{HH}$ = −3.2, $^1J_{RhH}$ = 19.0 and 29.0, $^2J_{PH}$ = 15.5 and 30.0, $^2J_{HCO}$ = 2.6) −17.60 (ddt, $^2J_{HH}$ = −3.2, $^1J_{RhH}$ = 24.8, $^2J_{PH}$ = 15.5)
3-[Br-H-Me]	$(PMe_3)_2BrHRh(\mu\text{-}Br)(\mu\text{-}H)Rh(CO)(PMe_3)$	318	−16.22 (ddddt, $^2J_{HH}$ = −3.8, $^1J_{RhH}$ = 19.1 and 30.2, $^2J_{PH}$ = 16.2 and 32) −16.72 (ddt, $^2J_{HH}$ = −3.8, $^1J_{RhH}$ = 24.0, $^2J_{PH}$ = 16.5)
3-[I-H-Me]	$(PMe_3)_2IHRh(\mu\text{-}I)(\mu\text{-}H)Rh(CO)(PMe_3)$	343	−14.46 (ddddt, $^2J_{HH}$ = −3.5, $^1J_{RhH}$ = 19.0 and 30.0, $^2J_{PH}$ = 14 and 32, $^2J_{HCO}$ = 3) −14.63 (ddt, $^2J_{HH}$ = −3.5, $^1J_{RhH}$ = 23, $^2J_{PH}$ = 15.5)
3-[H-I-Me]	$(PMe_3)_2IHRh(\mu\text{-}I)(\mu\text{-}H)Rh(CO)(PMe_3)$	328	−16.73 (ddddt, $^2J_{HH}$ = −3.5, $^1J_{RhH}$ = 31.5 and 16.7, $^2J_{PH}$ = 14 and 13.5, $^2J_{HCO}$ = 11) −14.80 (ddt, $^2J_{HH}$ = −3.5, $^1J_{RhH}$ = 21, $^2J_{PH}$ = 16)
4-[H-I-I-Me]	$(PMe_3)_2HRh(\mu\text{-}H)(\mu\text{-}I)_2Rh(CO)(PMe_3)$		−11.18 (dddt, $^2J_{HH}$ = −6, $^1J_{RhH}$ = 19 and 19, $^2J_{PH}$ = 99.5, 21 and 16) −14.75 (dddt, $^2J_{HH}$ = −6, $^1J_{RhH}$ = 28, $^2J_{PH}$ = 15 and 15)

[a] In C_6D_6 solution.

δ −16.35 and −16.72 are well separated. Spectral data for **2-[Cl-Cl-Ph]**, **2-[Br-Br-Ph]** and **2-[I-I-Ph]** can be found in Table 1. The dependence of the chemical shifts of both hydrides on the halide ligand of the precursor confirms their relative orientation in the reaction product.

Mechanism of binuclear product formation

The proposed mechanism of formation of complex **2** is outlined in Scheme 1. It begins with initial oxidative addition of

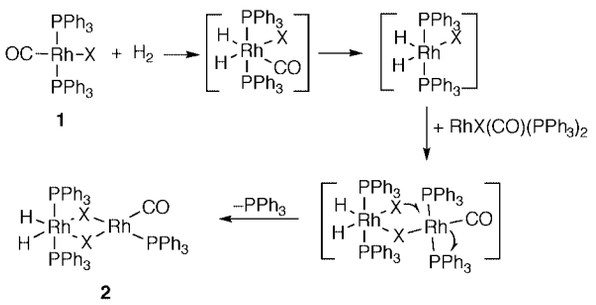

Scheme 1

H_2 to **1**. Even with the signal enhancement of PHIP, the initial dihydrogen activation product, $RhH_2X(CO)(PPh_3)_2$ [X = Cl, Br or I], is not detected in these experiments, probably due to facile CO loss and generation of the unsaturated species $RhH_2X(PPh_3)_2$. This is supported by the fact that when the analogous iridium complex, $IrH_2Cl(CO)(PPh_3)_2$, formed by H_2 oxidative addition to Vaska's complex, is warmed in the presence of PPh_3 both $IrH_2Cl(CO)(PPh_3)_2$ and $IrH_2Cl(PPh_3)_3$ are observed as parahydrogen enhanced products.[21,33] In order to prove that the generation of $IrH_2Cl(PPh_3)_3$ occurs *via* H_2 addition to $IrCl(CO)(PPh_3)_2$ followed by hydride labilisation of CO in the product $IrH_2Cl(CO)(PPh_3)_2$ rather than initial substitution of CO for phosphine in $IrCl(CO)(PPh_3)_2$ an additional control experiment was undertaken. This involved treating a sample of $IrCl(CO)(PPh_3)_2$ with an excess of PPh_3 before adding p-H_2 and monitoring by NMR spectroscopy. These spectra revealed that both samples generated $IrH_2Cl(PPh_3)_3$ at the same rate, indicating that the reaction proceeds *via* H_2 attack on $IrCl(CO)(PPh_3)_2$ rather than $IrCl(PPh_3)_3$.

After generation of the co-ordinatively unsaturated species $RhH_2X(PPh_3)_2$ in Scheme 1, the next step in binuclear product formation most likely involves attack on the unsaturated rhodium(III) centre by an electron pair of the halide ligand of unchanged $RhX(CO)(PPh_3)_2$. The resultant binuclear intermediate then forms **2** by generation of a second halide bridge from the rhodium(III) to the rhodium(I) centre with concomitant or subsequent PPh_3 loss.

For the observation of **2-[Cl-Cl-Ph]** and **2-[Br-Br-Ph]**, samples containing the corresponding precursor must first be warmed to temperatures in excess of 333 K, while for **2-[I-I-Ph]** 313 K is sufficient. This temperature differential for reaction allowed us to probe further the mechanism of formation of the binuclear complexes since in a mixed sample of **1-[I-Ph]** and **1-[Cl-Ph]** or **1-[Br-Ph]** at 313 K only **1-[I-Ph]** reacts with H_2 to form $RhH_2I(PPh_3)_2$ selectively. Binuclear complex formation can then be probed through competitive trapping of $RhH_2I(PPh_3)_2$ by unchanged **1-[I-Ph]** or by **1-[Cl-Ph]** or **1-[Br-Ph]**. Samples were therefore prepared containing varying amounts of **1-[Cl-Ph]** (or **1-[Br-Ph]**) and **1-[I-Ph]** and the reaction with p-H_2 at 313 K was monitored by NMR spectroscopy. When the ratio of **1-[Cl-Ph]** to **1-[I-Ph]** was 1:1, the corresponding ^1H spectrum contained hydride resonances for **2-[I-I-Ph]**, and an additional dihydride product at δ −16.57 and −19.58 denoted as **2-[I-Cl-Ph]**. A ^{31}P decoupled ^1H–^1H COSY spectrum confirmed that these two resonances were coupled. Furthermore, these resonances possess the same fine structure as those of

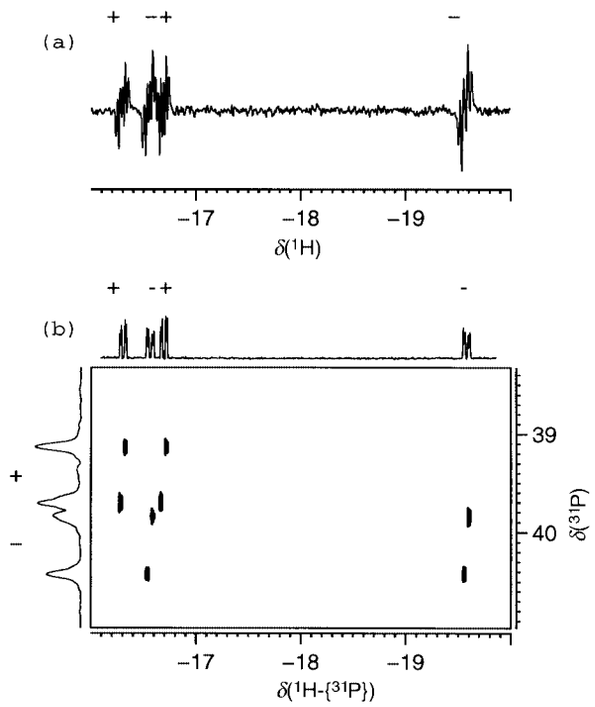

Fig. 2 The NMR spectra of the products **2-[I-I-Ph]** and **2-[Cl-I-Ph]** formed by warming $RhCl(CO)(PPh_3)_2$, **1-[Cl-Ph]**, and $RhI(CO)(PPh_3)_2$, **1-[I-Ph]**, in the ratio 8:1 with p-H_2 in C_6D_6 at 313 K: (a) ^1H spectrum showing the hydride resonances; (b) selected cross peaks (absolute value display) and projections in the ^1H–^{31}P HMQC correlation spectrum showing hydride and phosphorus chemical shift connections (^{31}P decoupled).

2-[Cl-Cl-Ph] and **2-[I-I-Ph]**, namely a doublet of triplets of anti-phase doublets multiplicity. When the ratio of **1-[Cl-Ph]** to **1-[I-Ph]** was increased to 8:1 the hydride resonances of **2-[I-I-Ph]** and the new product **2-[I-Cl-Ph]** are of equal intensity at 313 K, and no signals are detected that can be attributed to **2-[Cl-Cl-Ph]** (Fig. 2a). We have already seen that hydride ligands *trans* to chloride in **2-[Cl-Cl-Ph]** resonate at $\delta \approx -19.5$, while those *trans* to iodide in **2-[I-I-Ph]** are found at $\delta \approx -16.5$. The chemical shifts of the hydride resonances of **2-[I-Cl-Ph]** (δ −16.57 and −19.58) indicate that the product must contain both iodide and chloride bridges with hydrides *trans* to each. We therefore assign these resonances to the complex $(PPh_3)_2H_2Rh(\mu\text{-}Cl)(\mu\text{-}I)(CO)Rh(PPh_3)$, **2-[I-Cl-Ph]**.

Fig. 2(b) illustrates the ^1H–^{31}P HMQC spectrum of the sample containing the chloride and iodide complexes **1-[Cl-Ph]** and **1-[I-Ph]**, respectively, under p-H_2. Utilisation of a second dimension, in this case ^{31}P, helps separate the overlapping hydride resonances, and substantially aids spectral interpretation. When this process is repeated with **1-[Br-Ph]** and **1-[I-Ph]** four hydride resonances belonging to **2-[I-I-Ph]** and the new mixed halide product $(PPh_3)_2H_2Rh(\mu\text{-}Br)(\mu\text{-}I)Rh(CO)(PPh_3)$, **2-[I-Br-Ph]**, were detected. In this case, for equal ratios of **1-[Br-Ph]** and **1-[I-Ph]** the hydride signal intensity ratio of **2-[I-I-Ph]** to **2-[I-Br-Ph]** is 7:1. The relative rates of precursor attack on $RhH_2I(PPh_3)_2$ can be estimated from the hydride signal intensities and the precursor ratios assuming that the concentrations of the binuclear products are so low that the ratio of **1-[Br-Ph]** and **1-[I-Ph]** approximates to the initial ratio. These data reveal that the rate of trapping of $RhH_2I(PPh_3)_2$ by the iodide of $RhI(CO)(PPh_3)_2$ is 7 times faster than with the bromide ligand of **1-[Br-Ph]**, and 8 times faster than with the chloride ligand of **1-[Cl-Ph]**.

Close examination of Scheme 1 reveals that for mixtures of $RhI(CO)(PPh_3)_2$ and $RhX(CO)(PPh_3)_2$ there are two possible geometries available to the binuclear Rh^{III}–Rh^{I} dihydrides product differing only in the orientation of the CO and PPh_3 ligands at the rhodium(I) centre relative to the μ-iodide group.

Table 2 ^{31}P NMR Data for complexes **2**–**4**[a]

Complex	Formula	δ, (J/Hz)
2-[Cl-Cl-Ph]	$(PPh_3)_2H_2Rh(\mu\text{-}Cl)_2Rh(CO)(PPh_3)$	40.0 ($^1J_{RhP}$ = 118)
2-[Br-Br-Ph]	$(PPh_3)_2H_2Rh(\mu\text{-}Br)_2Rh(CO)(PPh_3)$	39.7 ($^1J_{RhP}$ = 115)
2-[I-I-Ph]	$(PPh_3)_2H_2Rh(\mu\text{-}I)_2Rh(CO)(PPh_3)$	39.4 ($^1J_{RhP}$ = 117)
2-[I-Cl-Ph]	$(PPh_3)_2H_2Rh(\mu\text{-}Cl)(\mu\text{-}I)Rh(CO)(PPh_3)$	40.1 ($^1J_{RhP}$ = 120)
2-[I-Br-Ph]	$(PPh_3)_2H_2Rh(\mu\text{-}Br)(\mu\text{-}I)Rh(CO)(PPh_3)$	39.9 ($^1J_{RhP}$ = 120)
2-[Br-Cl-Ph]	$(PPh_3)_2H_2Rh(\mu\text{-}Cl)(\mu\text{-}Br)Rh(CO)(PPh_3)$	40.0 ($^1J_{RhP}$ = 117)
2-[Cl-Br-Ph]	$(PPh_3)_2H_2Rh(\mu\text{-}Cl)(\mu\text{-}Br)Rh(CO)(PPh_3)$	39.5 ($^1J_{RhP}$ = 115)
2-[I-I-Me]	$(PMe_3)_2H_2Rh(\mu\text{-}I)_2Rh(PMe_3)(CO)$	−16.4 ($^1J_{RhP}$ = 104)
3-[Cl-H-Me]	$(PMe_3)_2ClHRh(\mu\text{-}Cl)(\mu\text{-}H)Rh(CO)(PMe_3)$	−1.5 ($^1J_{RhP}$ = 160); −5.7 ($^1J_{RhP}$ = 120)[b]
3-[Br-H-Me]	$(PMe_3)_2BrHRh(\mu\text{-}Br)(\mu\text{-}H)Rh(CO)(PMe_3)$	−3.7 ($^1J_{RhP}$ = 155); −10.5 ($^1J_{RhP}$ = 92)[b]
3-[I-H-Me]	$(PMe_3)_2HIRh(\mu\text{-}I)(\mu\text{-}H)Rh(CO)(PMe_3)$	−6.0 ($^1J_{RhP}$ = 155); −15.9 ($^1J_{RhP}$ = 96)[b]
3-[H-I-Me]	$(PMe_3)_2HIRh(\mu\text{-}H)(\mu\text{-}I)Rh(CO)(PMe_3)$	−0.6 ($^1J_{RhP}$ = 151); −16.5 ($^1J_{RhP}$ = 97)[b]
4-[H-H-I-Me]	$(PMe_3)_2HRh(\mu\text{-}H)(\mu\text{-}I)_2Rh(CO)(PMe_3)$	−10.34 (*trans* to hydride, $^1J_{RhP}$ = 120, $^4J_{PP}$ = 70 and 40) 0.6 ($^1J_{RhP}$ = 145, $^4J_{PP}$ = 70) 10.38 ($^1J_{RhP}$ = 126, $^2J_{PP}$ = 40)

[a] In C_6D_6 solution. [b] Large and small couplings indicative of Rh^I and Rh^{III}.

Table 3 ^{103}Rh NMR Data for complexes **2**–**4**[a]

Complex	Formula	δ
2-[Cl-Cl-Ph]	$(PPh_3)_2H_2Rh(\mu\text{-}Cl)_2Rh(CO)(PPh_3)$	925
2-[Br-Br-Ph]	$(PPh_3)_2H_2Rh(\mu\text{-}Br)_2Rh(CO)(PPh_3)$	345
2-[I-I-Ph]	$(PPh_3)_2H_2Rh(\mu\text{-}I)_2Rh(CO)(PPh_3)$	32
2-[I-Cl-Ph]	$(PPh_3)_2H_2Rh(\mu\text{-}Cl)(\mu\text{-}I)Rh(CO)(PPh_3)$	281
2-[I-Br-Ph]	$(PPh_3)_2H_2Rh(\mu\text{-}Br)(\mu\text{-}I)Rh(CO)(PPh_3)$	198
2-[Br-Cl-Ph]	$(PPh_3)_2H_2Rh(\mu\text{-}Cl)(\mu\text{-}Br)Rh(CO)(PPh_3)$	423
2-[Cl-Br-Ph]	$(PPh_3)_2H_2Rh(\mu\text{-}Cl)(\mu\text{-}Br)Rh(CO)(PPh_3)$	420
2-[I-I-Me]	$(PMe_3)_2H_2Rh(\mu\text{-}I)_2Rh(CO)(PMe_3)$	74
3-[Cl-H-Me]	$(PMe_3)ClHRh(\mu\text{-}Cl)(\mu\text{-}H)Rh(CO)(PMe_3)$	347, −688[b]
3-[Br-H-Me]	$(PMe_3)_2BrHRh(\mu\text{-}Br)(\mu\text{-}H)Rh(CO)(PMe_3)$	182, −69[b]
3-[I-H-Me]	$(PMe_3)_2IHRh(\mu\text{-}I)(\mu\text{-}H)Rh(CO)(PMe_3)$	−210, −733[b]

[a] In C_6D_6 solution. [b] Chemical shifts indicative of Rh^{III} and Rh^I.

Collectively, the NMR data for the mixed systems described above confirm that $RhH_2I(PPh_3)_2$ reacts with either $RhCl(CO)(PPh_3)_2$, **1-[Cl-Ph]**, or $RhBr(CO)(PPh_3)_2$, **1-[Br-Ph]**, to form in each case only a single additional product.† The selectivity shown by this simple reaction is explained in more detail later.

On the basis of their individual reactivity profiles, warming **1-[Cl-Ph]** and **1-[Br-Ph]** together should yield both $RhH_2Cl(PPh_3)_2$ and $RhH_2Br(PPh_3)_2$, and the trapping of either of these co-ordinatively unsaturated species with **1-[Cl-Ph]** or **1-[Br-Ph]** should be possible. If this premise is valid, four products **2-[Cl-Cl-Ph]**, **2-[Br-Br-Ph]** and both μ-chloride-μ-bromide isomers **2-[Cl-Br-Ph]** and **2-[Br-Cl-Ph]** should be detected in the reaction. This was confirmed by the observation of four pairs of polarised hydride resonances in the corresponding ^{1}H NMR spectrum. The chemical shifts of the hydride resonances of two of these pairs match those of **2-[Cl-Cl-Ph]** and **2-[Br-Br-Ph]**, while those of the remaining pairs, at δ −18.43 and −19.58, and δ −18.54 and −19.33, suggest the presence of both Br and Cl bridges in each of the other two products. All of these resonances possess the same doublet of triplets of antiphase doublets multiplicity that has been observed for the other complexes in this series. In this reaction we are therefore able to form both isomers of the μ-chloride-μ-bromide product.

Tables 1–3 list the spectroscopic features of complexes **2**. The phosphorus chemical shifts for PPh_3 bound to the rhodium(III) centre are insensitive to the nature of the halide bridge, but the hydride and rhodium chemical shifts are dramatically affected. Thus, the ^{103}Rh chemical shifts move from δ 925 to 32 as the bridges change along the series (μ-Cl)$_2$, (μ-Cl)(μ-Br), (μ-Cl)(μ-I), (μ-Br)$_2$, (μ-Br)(μ-I), (μ-I)$_2$. This ordering illustrates the effect of the hard/soft nature of the bridging ligands on ^{103}Rh chemical shift and hence the effective radius of rhodium d electrons, and parallels similar trends reported in the literature;[34] for example $RhF(CO)(PPh_3)_2$ (δ −148), $RhCl(CO)(PPh_3)_2$ (δ −369), $RhBr(CO)(PPh_3)_2$ (δ −421) and $RhI(CO)(PPh_3)_2$ (δ −532). The fact that the rhodium(III) centres of **2-[Br-Cl-Ph]** and **2-[Cl-Br-Ph]** have such similar chemical shifts (δ 423 and 420) supports their assignment as isomers of $(PPh_3)_2H_2Rh(\mu\text{-}Cl)(\mu\text{-}Br)Rh(CO)(PPh_3)$.

Reactions of $RhX(CO)(PMe_3)_2$ [X = Cl, Br or I] with hydrogen

When a C_6D_6 solution of $RhCl(CO)(PMe_3)_2$, **1-[Cl-Me]**, was monitored at 342 K under 3 atm of p-H_2 the ^{1}H NMR spectrum shown in Fig. 3 was obtained within 60 s. The spectrum contains two new resonances at δ −17.10 and −17.60 having antiphase components, one of which differs significantly in structure from those of **2-[Cl-Cl-Ph]**. When a ^{1}H-{^{31}P} NMR spectrum is collected the δ −17.60 resonance collapses into a doublet of antiphase doublets with a 24.8 Hz coupling corresponding to $^1J_{Rh\text{-}H}$, while the δ −17.10 resonance simplifies to a doublet of doublets of antiphase doublets with couplings 29.0, 19.0 and −3.2 Hz, respectively (Fig. 3b). This is consistent with the δ −17.60 signal from a terminal hydride and the δ −17.10 signal arising from a bridging hydride.

When this system is examined using the HMQC approach described earlier to record ^{31}P and ^{103}Rh chemical shift information two sets of phosphorus and rhodium environments are detected (Fig. 3c and 3d represent typical spectra). The phosphorus resonance at δ −5.7 connects to both the terminal

† Further ligand exchange products such as $(PPh_3)_2H_2Rh(\mu\text{-}Cl)(\mu\text{-}I)Rh(PPh_3)_2$, $(PPh_3)_2H_2Rh(\mu\text{-}Br)(\mu\text{-}I)Rh(PPh_3)_2$, $(PPh_3)_2H_2Rh(\mu\text{-}Cl)(\mu\text{-}I)Rh(CO)_2$ and $(PPh_3)_2H_2Rh(\mu\text{-}Br)(\mu\text{-}I)Rh(CO)_2$ which would be p-H_2 active are not observed.

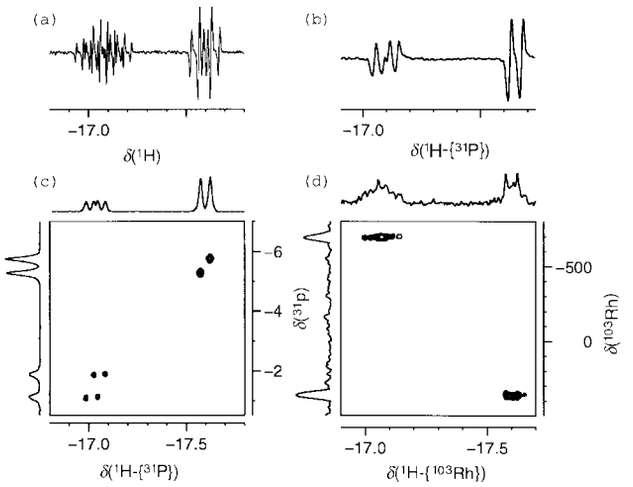

Fig. 3 The NMR spectra of the product **3-[Cl-H-Me]** formed by warming $RhCl(CO)(PMe_3)_2$, **1-[Cl-Me]**, with p-H_2 in C_6D_6 at 348 K: (a) ^1H spectrum showing the two hydride resonances; (b) ^1H-{^{31}P} spectrum showing the effect of removing ^{31}P couplings; (c) selected cross peaks (absolute value display) and projections in the ^1H–^{31}P HMQC correlation spectrum; ^{31}P decoupled); (d) selected cross peaks (absolute value display) and projections in the ^1H–^{103}Rh HMQC correlation spectrum.

and bridging hydride resonances and shows a doublet coupling to rhodium ($^1J_{RhP} = 120$ Hz). The phosphorus resonance at δ −1.5 also appears as a rhodium coupled doublet ($^1J_{RhP} = 160$ Hz), but it only connects to the bridging hydride resonance. The values of $^1J_{Rh(III)P}$ and $^1J_{Rh(I)P}$ reported for $(P^iPr_3)_2H_2Rh(\mu\text{-}Cl)_2Rh(P^iPr_3)_2$ are 113 and 194 Hz respectively while those for $(P^iPr_3)_2H_2Rh(\mu\text{-}Cl)_2Rh(P^iPr_3)(C_8H_{14})$ are 114 and 182 Hz.[35] Consequently, the difference in $^1J_{RhP}$ for the two p-H_2 enhanced resonances, 120 and 160 Hz, is consistent with their attachment to rhodium centres in the +I and +III oxidation states. These data are consistent with the fact that, when a ^1H NMR spectrum is obtained while selectively decoupling the ^{31}P resonance at δ −5.7, the δ −17.60 resonance collapses into a doublet of antiphase doublets (rhodium and hydride) while the δ −17.10 resonance simplifies to a doublet of triplets of antiphase doublets (split by two rhodium, one phosphorus and one proton nuclei). In the corresponding ^1H–^{103}Rh HMQC experiments cross peaks were observed which connect the bridging hydride resonance at δ −17.10 to rhodium resonances at δ 347 and −688 and the terminal hydride resonance to the resonance at δ 347. These data confirm that the resonance at δ 347 arises from the rhodium(III) centre while that at δ −688 corresponds to the rhodium(I) centre. The efficiency of cross-peak formation in such HMQC experiments depends critically on the size of the active coupling (J_{PH} or J_{RhH}) because they employ a delay, which should be set to $1/2J$, to achieve optimum coherence transfer.[12] In view of the fact the solution to $1/2J$ is not unique, several experiments, with different delays, were necessary to see all connections and hence ensure the accuracy of these assignments. When the H_2 addition reaction to **1-[Cl-Me]** is repeated with ^{13}CO-labelled $RhCl(CO)(PMe_3)_2$, the δ −17.10 hydride resonance clearly shows an additional doublet coupling ($^2J_{HC} = 2.6$ Hz) in the ^1H-{^{31}P} spectrum, whereas the δ −17.60 resonance is unaffected by the labelling. Furthermore, a ^1H–^{13}C HMQC experiment connects the δ −17.10 hydride resonance to a ^{13}CO resonance at δ 189.3 which is split by ^{31}P and ^{103}Rh nuclei.

The NMR results thus reveal that the hydride resonance at δ −17.60 is coupled to a single rhodium centre, two equivalent phosphines and the second hydride. From the magnitude of the coupling constants, the two phosphines and the other hydride are in *cis* positions. The more complex hydride resonance at δ −17.10 couples to the same Rh and P nuclei while possessing additional couplings to a second, inequivalent

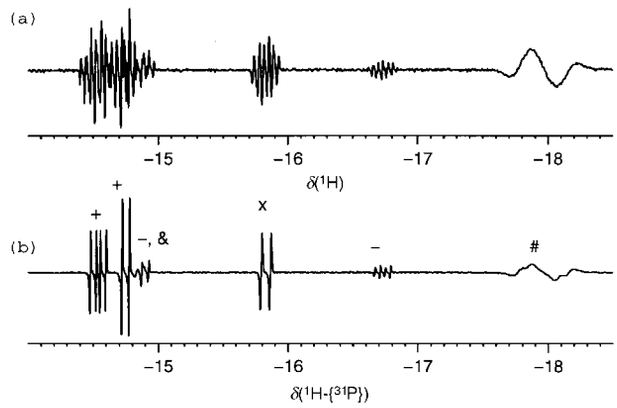

Fig. 4 The NMR spectra of the products formed by warming $RhI(CO)(PMe_3)_2$, **1-[I-Me]**, with p-H_2 in C_6D_6 at 343 K: (a) ^1H spectrum showing selected hydride resonances of **3-[I-H-Me]**(+), **3-[H-I-Me]**(−), **2-[I-I-Me]**(#) and **4-[H-I-I-Me]**(&) (x = $RhH_2Cl(PMe_3)_3$); (b) ^1H-{^{31}P} spectrum, doublet of antiphase doublet multiplicity indicates terminal hydride resonance, while doublet of doublet of antiphase doublets indicates bridging hydride.

rhodium centre, to a single phosphine ligand co-ordinated to that centre, and when **1-[Cl-Me]**-^{13}CO is used to a *cis* carbonyl ligand. Based on these results, it is possible to assign the structure of the product observed in the reaction of $RhCl(CO)(PMe_3)_2$ with hydrogen as $(PMe_3)_2(Cl)HRh(\mu\text{-}H)(\mu\text{-}Cl)Rh(CO)(PMe_3)$, **3-[Cl-H-Me]**.

When this process is repeated with $RhBr(CO)(PMe_3)_2$, **1-[Br-Me]**, the product $(PMe_3)_2(Br)HRh(\mu\text{-}H)(\mu\text{-}Br)Rh(CO)(PMe_3)$, **3-[Br-H-Me]**, was most readily characterised.‡ The bridging hydride ligand of **3-[Br-H-Me]** resonates at δ −16.22 while the terminal hydride appears at δ −16.72. Both of these ^1H resonances possess similar multiplicities to those described for **3-[Cl-H-Me]**.

However, when a C_6D_6 solution of $RhI(CO)(PMe_3)_2$, **1-[I-Me]**, is monitored by ^1H NMR spectroscopy at 348 K while under 3 atm of p-H_2 the spectrum shown in Fig. 4(a) is obtained. Close examination reveals the presence of ten p-H_2 enhanced hydride resonances belonging to five reaction products. In the corresponding ^1H-{^{31}P} NMR spectrum, seven of these resonances, at δ −10.00, −14.63, −14.75, −14.80, −15.83, −17.70, and −18.02, simplify into doublets of antiphase doublets, while three, at δ −11.18, −14.46 and −16.73, become doublets of doublets of antiphase doublets (Fig. 4b). This indicates that the first group of resonances correspond to terminal hydride ligands while the latter correspond to bridging hydride ligands. The connectivity of these hydrides was established by a gradient assisted ^1H–^1H-{^{31}P} correlation spectrum (COSY) (Fig. 5a).

At 348 K the most intense signals originate from the mutually coupled pair of hydride resonances at δ −14.46 and −14.63 which can be shown to arise from the iodo- and hydrido-bridged complex $(PMe_3)_2(I)(H)Rh(\mu\text{-}H)(\mu\text{-}I)Rh(CO)(PMe_3)$, **3-[I-H-Me]**. The NMR data for **3-[I-H-Me]** are presented in Tables 1–4. The ^1H–^{31}P HMQC experiment (Fig. 5b) reveals that the hydride partner at δ −14.46, identified above as bridging, couples to two separate sets of ^{31}P nuclei, which are themselves not coupled, at δ −6.0 ($^2J_{PH} = 14$, $^1J_{RhP} = 155$ Hz) and −15.9 ($^2J_{PH} = 32$, $^1J_{RhP} = 96$ Hz), respectively. When compound **1-[I-Me]** was specifically labelled with ^{13}CO the resonance due to the bridging hydride possessed an additional coupling of 3 Hz and correlates with a ^{13}C resonance at δ 185.8 in the corresponding ^1H–^{13}C HMQC spectrum.

A minor reaction product possessing similar spectral features to those of **3-[I-H-Me]** is also observed in the reaction. The hydride resonances appear at δ −14.80 and −16.73, but the

‡ Weak resonances with spectral features similar to those of complexes **2-[I-I-Me]** and **4-[H-I-I-Me]** are also visible.

Table 4 ^{13}C NMR Data for complexes **3**[a]

Complex	Formula	δ (J/Hz)
3-[Cl-H-Me]	$(PMe_3)_2ClHRh(\mu\text{-}Cl)(\mu\text{-}H)Rh(CO)(PMe_3)$	189.3 ($^2J_{PC}$ = 18.6, $^1J_{RhC}$ = 75.0)
3-[Br-H-Me]	$(PMe_3)_2BrHRh(\mu\text{-}Br)(\mu\text{-}H)Rh(CO)(PMe_3)$	188.0 ($^2J_{PC}$ = 18.7, $^1J_{RhC}$ = 77.6)
3-[I-H-Me]	$(PMe_3)_2IHRh(\mu\text{-}I)(\mu\text{-}H)Rh(CO)(PMe_3)$	185.8 ($^2J_{PC}$ = 16.9, $^1J_{RhC}$ = 79.8)

[a] In C_6D_6 solution. [b] Precursors to complexes labelled with ^{13}CO.

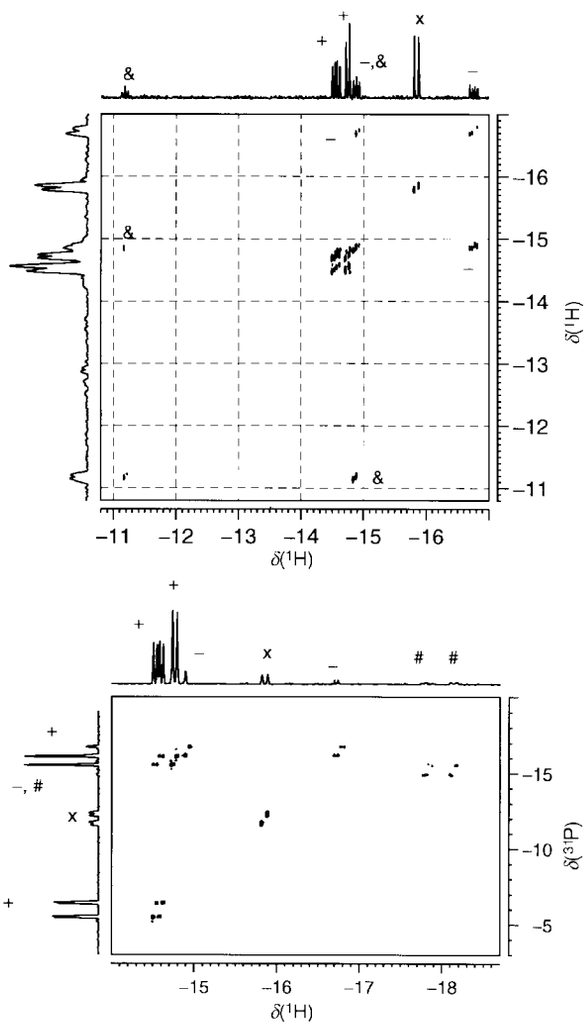

Fig. 5 The 2-D NMR spectra of the products formed by warming $RhI(CO)(PMe_3)_2$, **1-[I-Me]**, with p-H_2 in C_6D_6 at 343 K: (a) selected cross peaks (absolute value display) and projections in the ^1H–^1H COSY spectrum of **3-[I-H-Me]**(+), **3-[H-I-Me]**(−), **2-[I-I-Me]**(#) and **4-[H-I-I-Me]**(&) (x = $RhH_2Cl(PMe_3)_3$, ^{31}P decoupled); (b) selected cross peaks (absolute value display) and projections in the ^1H–^{31}P HMQC correlation spectrum (^{31}P decoupled), details as in (a).

phosphorus couplings to the bridging hydride are 13.5 and 14 Hz, while the hydride coupling to ^{13}CO increases to 11 Hz. The decrease in $^2J_{PH}$ from 32 to 13.5 Hz and corresponding increase in $^2J_{CH}$ from 3 to 11 Hz are consistent with the view that in the minor product, **3-[H-I-Me]**, the bridging hydride is *trans* to the CO ligand of the rhodium(I) centre rather than *trans* to the PMe_3 group, as in **3-[I-H-Me]**.

At 313 K the remaining resonances become sharper and hence easier to monitor. Four of these resonances are assigned to the products $(PMe_3)_2H_2Rh(\mu\text{-}I)_2Rh(CO)(PMe_3)$, **2-[I-I-Me]**, and $RhH_2I(PMe_3)_3$. The mutually coupled hydride resonances of **2-[I-I-Me]** appear at δ −17.70 and −18.02, and possess additional couplings due to one rhodium and two phosphorus nuclei, the resonances of which were located at δ 74 and −16.4 ($^1J_{RhP}$ =104 Hz) in the corresponding ^1H–^{103}Rh and ^1H–^{31}P HMQC experiments, respectively. Although couplings to iodide are not visible, evidence for the iodide bridges comes directly from the chemical shifts of the hydrides ligands of **2-[I-I-Me]** at δ −17.70 and −18.02 which require the presence of *trans* electronegative ligands as seen in **2**. Additionally, the rhodium chemical shift, δ 74, is similar to that of δ 32 observed for **2-[I-I-Ph]**.

A final product obtained from complex **1-[I-Me]** contains two hydride resonances at δ −11.18 and −14.75. The former possesses a large phosphorus coupling, $^2J_{PH}$ = 99.5 Hz, indicative of a *trans* H–PMe_3 arrangement, two additional couplings to other phosphorus nuclei, J_{PH} = 21 and 16 Hz, and essentially equal couplings to two rhodium centres, $^1J_{RhH}$ = 19 Hz, consistent with a bridge position. The resonance at δ −14.75 exhibits doublets of triplets of antiphase doublets coupling similar to the terminal hydride ligands seen for complexes **2** and **3**. Based on the chemical shift and coupling data including the *trans* J_{PH} for the bridging hydride along with two other *cis* J_{PH} couplings, we propose that the structure shown as **4-[H-I-I-Me]** is assigned. When $RhI(^{13}CO)(PMe_3)_2$ is employed no additional hydride–^{13}C couplings are visible; however, the resonance linewidth is sufficient to hide a small *cis* coupling suggesting that the bridging hydride in **4-[H-I-I-Me]** is most likely located *cis* to the carbonyl of the second rhodium (1.5) centre. As additional support for this assignment, we note that in the complexes $Rh_2(\mu\text{-}H)_2\{P[N(CH_3)_2]_3\}_4$ and $Rh_2(\mu\text{-}H)_2\{P[O\text{-}i\text{-}C_3H_7]_3\}_4$, containing rhodium(I) centres with near coplanar framework atoms $P_2Rh(\mu\text{-}H)_2P_2$, reported by Muetterties and co-workers, the corresponding H_{bridge}–P couplings are established at around 30 Hz.[36,37] The related complex $\{P(O\text{-}i\text{-}C_3H_7)_3\}_2(\mu\text{-}H)_2HRh(\mu\text{-}H)Rh\{P(O\text{-}i\text{-}C_3H_7)_3\}_2$ has been reported to possess hydride resonances at δ −7.8 (J_{PH} = 180, 2 H), −11.1 (J_{PH} = 89 Hz, 1H) and –14.5 (1H).[10]

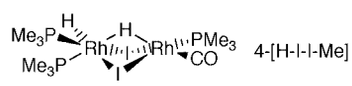

4-[H-I-I-Me]

Chart 3

Binuclear product selection

Close examination of the chemical shift data provided by **3-[I-H-Me]** and **3-[H-I-Me]** enables the locations of the CO and phosphine ligands of the rhodium(I) centres of the binuclear products to be identified. Specifically, the terminal hydride of **3-[H-I-Me]**, which is located *trans* to μ-iodide that is in turn *trans* to phosphine at Rh^I, appears at δ −14.80, while that of isomer **3-[I-H-Me]** which is *trans* to μ-iodide that is in turn *trans* to CO appears at δ −14.46. The chemical shift of the terminal hydride is therefore influenced by the electron donating ability of the bridging halide which in turn is maximised when *trans* to phosphine. To simplify the structural descriptions of the binuclear complexes with regard to the relative orientation of the terminal hydrides at Rh^{III} and the non-bridging ligands at Rh^I, we say that in **3-[I-H-Me]** the terminal hydride is *cisoid* to CO whereas in **3-[H-I-Me]** it is *cisoid* to PMe_3 on Rh^I.

Based on the effect that the bridging halide has on the chemical shift of the hydride resonances, we can assign the hydride resonances of the PPh_3 complexes **2** and analyse more deeply their selectivity of formation. From their chemical shifts,

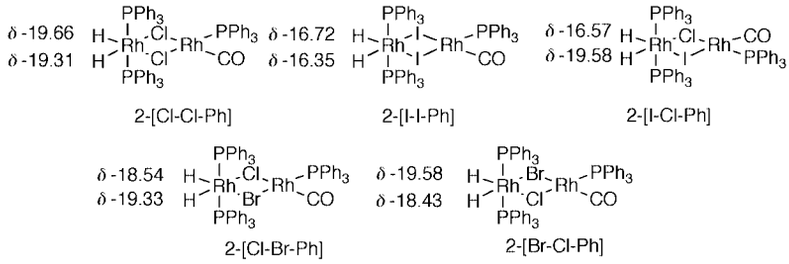

Chart 4

the hydride resonance of **2-[Cl-Cl-Ph]** at δ −19.66 can be assigned to the hydride ligand *cisoid* to PPh_3 on Rh^I, while the hydride ligand at δ −19.31 is *cisoid* to the carbonyl ligand. This simple analysis can be repeated for **2-[Br-Br-Ph]** and **2-[I-I-Ph]**. In the cases of **2-[I-Cl-Ph]**, **2-[I-Br-Ph]**, **2-[Cl-Br-Ph]** and **2-[Br-Cl-Ph]** extension of this analysis enables the geometries of the associated mixed halide products to be assigned. The chemical shifts of the hydride resonances of **2-[Cl-Cl-Ph]**, **2-[I-Cl-Ph]**, and **2-[Br-Cl-Ph]** that are *trans* to the chloride bridge and *cisoid* to the phosphine on Rh^I appear at around δ −19.6, whereas the resonances of **2-[Cl-Cl-Ph]** and **2-[Cl-Br-Ph]** that appear at *ca.* δ −19.3 are consistent with a hydride ligand that is *trans* to the corresponding chloride bridge and *cisoid* to the carbonyl ligand. The chemical shift assignments for each hydride are summarised above.

We now return to the question of product selectivity in the reaction systems containing mixtures of **1-[I-Ph]** + **1-[Cl-Ph]** and **1-[I-Ph]** + **1-[Br-Ph]**. In each reaction system, only one mixed halide binuclear product was observed despite the fact that two possible di-μ-halide products can be envisioned as shown in Scheme 2. Through use of the chemical shift data for

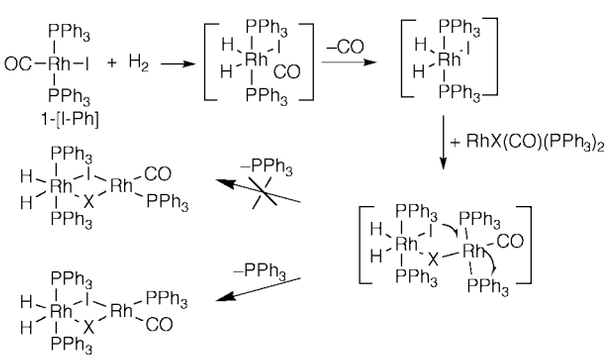

Scheme 2

the hydrides of **2-[I-Cl-Ph]** and **2-[I-Br-Ph]** to determine which hydride is *trans* to each halide and which is *cisoid* to CO on the rhodium(I) centre, the selectivity of product formation can be analysed more deeply. The key step(s) in this regard involves generation of the second halide bridge using iodide originally bound to Rh^{III} with subsequent loss of PPh_3 from the rhodium(I) centre. In each case, therefore, the halide of the original rhodium(I) complex that activated H_2 ends up *trans* to the CO ligand of the rhodium(I) centre (Scheme 2).

For the PMe_3 complexes **1-Me** the reactions with H_2 leading to products **3-[H-Cl-Me]** and **3-[H-I-Me]** are envisioned to proceed according to Scheme 3. The initial steps of the sequence oxidative addition of H_2 to **1-Me**, CO loss, and the formation of the initial halide bridge remain the same. Trapping of the unsaturated rhodium(III) species by unchanged **1-Me** is supported by the notion that as the concentration of **1-Me** is increased the NMR resonances arising from the mononuclear product $RhH_2X(PMe_3)_3$ decrease substantially. The bridge closure step for the PMe_3 system **1-[I-Me]** has three possibilities, one leading to a second iodide bridge as in **2-[I-I-Me]** and the

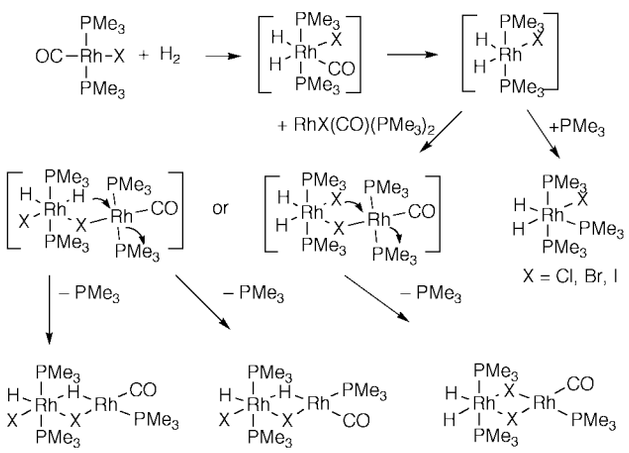

Scheme 3

other two leading to the μ-hydrido μ-iodo products **3-[I-H-Me]** and **3-[H-I-Me]**.

Theoretical comparisons

The diverse spectrum of products observed in these reactions prompted us to analyse the structures and stabilities of the bimetallic products using approximate density functional theory. The chloride, bromide and iodide systems were considered, and in each case the phosphine ligands were modelled by PH_3. For each of the three halides distinct minima were located on the potential energy surface, corresponding to each of the four structural types identified in the NMR studies, namely the dihalide-bridged species, **2-[X-X-H]**, the two isomers of the mixed hydride–halide bridged species, **3-[X-H-H]** and **3-[H-X-H]**, and the triply bridged species, **4-[X-X-H-H]**. The energies of the four isomers are summarised in Fig. 6. In all three systems the most stable isomer has the two halide ligands in the bridging positions, with two terminal hydrides. This is consistent with the observed chemistry of the triphenylphosphine species, where only the dihalide-bridged species is observed. The comparison between calculated and experimental results is rather more difficult for the trimethylphosphine analogues, because the broad signal observed for the dihalide-bridged species precludes an accurate determination of the relative concentrations of the different isomers. For the iodide complexes all four structures lie less than 12 kJ mol^{-1} above the most stable diiodide bridged isomer, consistent with the mixture of products observed in solution. Of the two mixed iodide/hydride-bridged species, that with the hydride *trans* to the PH_3 group, **3-[I-H-H]**, lies 6 kJ mol^{-1} lower in energy than the alternative with H *trans* to CO, **3-[H-I-H]**, again consistent with the observed signal strengths for **3-[I-H-Me]** and **3-[H-I-Me]**. The triply bridged species [**4-H-I-I-H**] is approximately iso-energetic with **3-[H-I-Me]**, thereby rationalising the detection of the triply bridged species in this case. For the chloride and bromide analogues the most stable product again corresponds to the dihalide bridged species, but the other isomers lie much higher in energy, and accordingly the

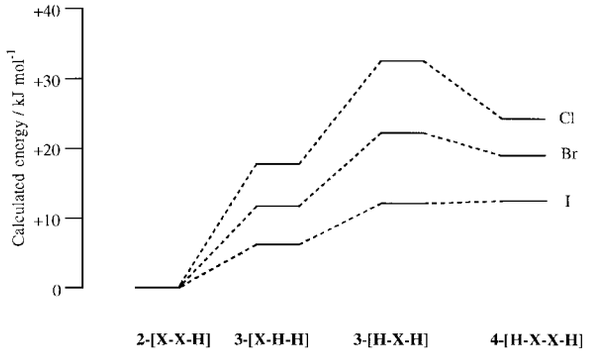

Fig. 6 Relative energies for the binuclear products **2-[X-X-H]**, **3-[X-H-H]**, **3-[H-X-H]** and **4-[H-X-X-H]** where X = Cl, Br or I.

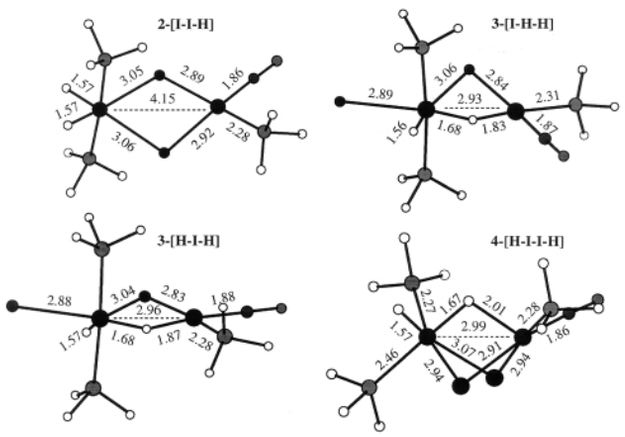

Fig. 7 Calculated structures and bond lengths (Å) for products **2-[I-I-H]**, **3-[I-H-H]**, **3-[H-I-H]** and **4-[H-I-I-H]**.

observed product distribution is less diverse. In each case the mixed halide/hydride-bridged species with the hydride *trans* to the PH_3 group, **3-[X-H-H]**, is the next most stable isomer, and **3-[X-H-Me]** is the dominant species observed in solution for PMe_3.

Optimised structural parameters for the four isomers of the iodide system are summarised in Fig. 7 (the important features are similar for X = Cl or Br). In the **2-[I-I-H]** isomer the co-ordination spheres of the metal centres are typical of octahedral Rh^{III} and square planar Rh^{I}. The Rh^{III}–Rh^{I} separation is long (4.15 Å), and the Rh^{III}–I bond lengths (3.05 Å) are somewhat longer than their Rh^{I}–I counterparts (2.85 Å) due to the strong *trans* influence of the hydride ligands on the Rh^{III} centre. In the two iodide/hydride bridged isomers the hydride bridge is highly asymmetric, with the ligand lying much closer to the rhodium(III) centre (1.68 Å) than to Rh^{I} (1.83–1.87 Å). Similar features are observed in the triply bridged species, **4-[I-I-H-H]**, with the Rh^{III}–H distance (1.67 Å) significantly shorter than its Rh^{I}–H counterpart (2.01 Å). The longer Rh^{I}–H bond in the latter arises because in the doubly bridged species the hydride ligand is required to complete the square planar co-ordination, whereas in the triply bridged isomer the rhodium(I) centre is already co-ordinatively saturated due to the presence of two iodide bridges. In the species where a hydride bridge is present the Rh–Rh separation is significantly shorter than in the di-μ-iodide species (*ca.* 2.96 *vs.* 4.15 Å). This brings the phosphine ligands on opposite ends of the molecule closer together, and the greater potential for steric interactions in the hydride-bridged isomers (either in the stable species described here or in the transition states leading to closure of the bridge) may account for the different product distributions seen for triphenyl- and trimethyl-phosphine systems. Calculations using the hybrid quantum mechanics/molecular mechanics methodology are currently being performed to analyse this possibility.

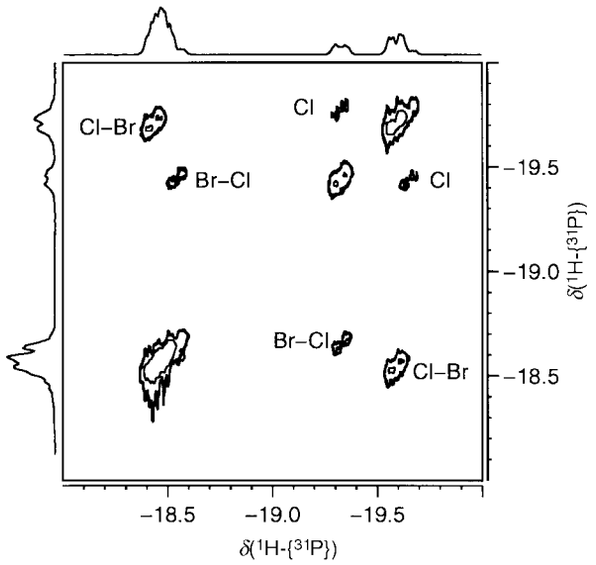

Fig. 8 The ^{1}H-$\{^{31}P\}$ EXSY spectrum (absolute value display) of a sample containing complexes **2-[Cl-Cl-Ph]**, **2-[Br-Br-Ph]**, **2-[Cl-Br-Ph]** and **2-[Br-Cl-Ph]**, formed by warming **1-[Cl-Ph]** and **1-[Br-Ph]** with p-H_2 in C_6D_6 at 316.6 K for a mixing time of 0.1 s. Exchange peaks connecting the hydride resonances of **2-[Cl-Cl-Ph]**, **2-[Cl-Br-Ph]** and **2-[Br-Cl-Ph]** are indicated.

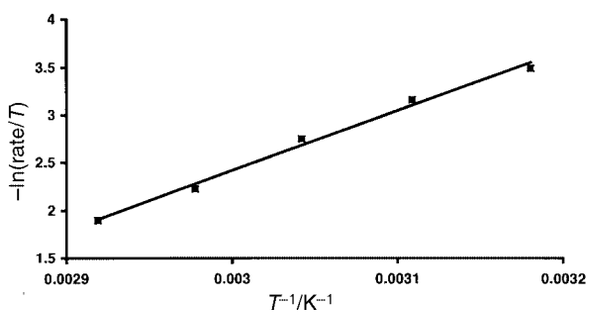

Fig. 9 Plot of $-\ln(\text{rate hydride interchange})/T$ *vs.* $1/T$ for complex **2-[Cl-Cl-Ph]** between the temperatures 315 and 345 K.

Intermolecular hydride exchange

The exchange spectroscopy (EXSY) experiment has been widely utilised to obtain information about internuclear distances and exchange processes.[8] We have shown that this approach can be used in conjunction with p-H_2 to probe the ligand sphere around the metal centre, and to monitor ligand exchange processes.[33] Here we also demonstrate that rates and activation parameters can be obtained for species detected through parahydrogen derived signals.[39]

When **1-[Cl-Ph]** is warmed with p-H_2 and monitored at 343 K positive exchange cross peaks are observed to connect the hydride resonances of the binuclear product **2-[Cl-Cl-Ph]** that were located on the diagonal. The observation of these cross peaks indicates that the hydride ligands of **2-[Cl-Cl-Ph]** exchange position during the mixing time associated with this experiment (Fig. 8). Spectra were recorded for a variety of mixing times, and using standard methods for a two-site exchange process the rate of hydride interchange, k_{obs}/s^{-1}, was extracted from the data.[25] The rate of hydride interconversion in **2-[Cl-Cl-Ph]** was determined to be 13.7 s^{-1} (obtained by extrapolation since **2-[Cl-Cl-Ph]** is not observed at 313 K) while the activation parameters $\Delta H^{\ddagger} = 52 \pm 9$ kJ mol^{-1} and $\Delta S^{\ddagger} = -61 \pm 27$ J K^{-1} mol^{-1} were obtained by analysing the rate data as a function of temperature (Fig. 9). This approach was repeated for each of the complexes **2** (because the hydride resonances of **2-[Br-Br-Ph]** appear as a second order multiplet no rate data were obtained for hydride interchange for this complex), and results

Table 5 Rate and activation parameter data for the interchange of the hydride ligands in the binuclear complexes **2**

Complex	Bridging atoms	Rates/s^{-1}, 313 K	$\Delta H^{\ddagger}$/kJ mol^{-1}	$\Delta S^{\ddagger}$/J K^{-1}
2-[Cl-Cl-Ph]	$(\mu\text{-Cl})_2$	13.7	52 ± 9	−61 ± 27
2-[I-I-Ph]	$(\mu\text{-I})_2$	2.5	58 ± 15	−53 ± 47
2-[I-Cl-Ph]	(μ-I)(μ-Cl)	14.8	42 ± 11	−90 ± 35
2-[I-Br-Ph]	(μ-I)(μ-Br)	10.7	57 ± 10	−43 ± 33
2-[Br-Cl-Ph]	(μ-Br)(μ-Cl)	8.2	77 ± 18	+14 ± 57
2-[Cl-Br-Ph]	(μ-Cl)(μ-Br)	6.7	73 ± 27	−1 ± 85
2-[I-I-Me]	$(\mu\text{-I})_2$	20	57 ± 5	−34 ± 17

are summarised in Table 5. On the timescale of these experiments no exchange peaks connected the hydride resonances to that of free hydrogen.

In the EXSY experiments recorded on samples using mixed precursors the only visible cross peaks connect hydride resonances originating from the same species. Furthermore, when hydride interchange for **2-[I-Cl-Ph]** was measured as a function of the ratio of **1-[Cl-Ph]**:**1-[I-Ph]** the rates obtained were identical within experimental error (ratio 8:1, rate 14.8; ratio 5:1, rate 13.4; and ratio 2:1, rate 13.0 s^{-1}). This strongly suggests that the hydride exchange process is intramolecular. The similarity in exchange rate constants at 313 K for complexes containing $(\mu\text{-Cl})_2$ and (μ-I)(Cl) linkages (13.7 and 14.8 s^{-1}) when compared with that for a $(\mu\text{-I})_2$ linkage (**2-[I-I-Ph]**, 2.5 s^{-1}) is most consistent with the suggestion that the μ-chloride bridge, *trans* to phosphine, rather than μ-iodide of **2-[I-Cl-Ph]** is involved in the reaction. A mechanism starting with the dissociative opening of the halide bridge *trans* to the phosphine of the rhodium(I) centre is shown in Scheme 4. We

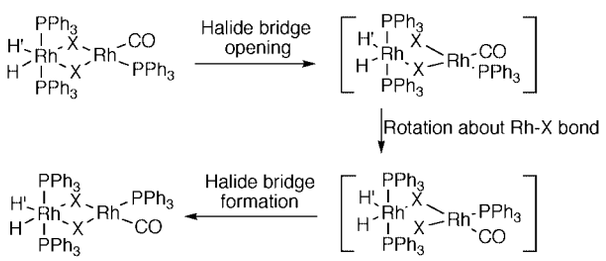

Scheme 4

expected this reaction therefore to have a positive entropy of activation, consistent with the increase in disorder associated with halide bridge opening. However, the experimentally determined negative entropy of activation implies that the reaction is more complex and a step which includes a degree of ordering is required. From the Scheme it is clear that once the singly bridged species is generated rotation about the remaining halide–Rh^{III} bond and hydride interchange *via* a trigonal-bipyramidal intermediate is required prior to reformation of the second bridge. Caulton and co-workers[40] have examined the related hydride interchange process for square pyramidal $IrH_2X(P^tBu_2R)_2$ [X = Cl, Br or I; R = Me or Ph] and found that the entropy of activation for this step is near zero. However, we note that solvent reorganisation or solvent co-ordination effects are also possible and that the final step of this process, bridge re-establishment, is clearly ordering in nature. The former option reflects the charge separation resulting from halide bond cleavage while the electron deficiency of both metal centres means that solvent co-ordination is also possible. Thus, in the light of the data presented here, the overall mechanism of hydride interchange, according to Scheme 4, is supported but an important role for the solvent cannot be excluded.

Intramolecular hydride exchange was also observed for **3-[Cl-H-Me]**, **3-[Br-H-Me]** and **3-[I-H-Me]** in the corresponding 2-D EXSY experiments. However, the rate of interchange for the bridging/terminal hydrides in **3-[I-H-Me]** was now dependent on the concentration of **1-[I-Me]**, with higher concentrations *suppressing* hydride interchange completely. These observations are consistent with hydride exchange at **3** proceeding *via* a more complex mechanism involving **1-[I-Me]**. If this process proceeds *via* Rh^{III}–halide bridge opening the Rh–H–Rh bond holding the two centres together will be very weak, and attack by the halide of **1-[I-Me]** may compete with total fragmentation. Such a process would ensure that the hydride ligands remain inequivalent, and at high concentrations account for the suppression of their interchange.

Conclusion

In this paper we have shown that the complexes $RhX(CO)(PR_3)_2$ [X = Cl, Br or I; R = Me or Ph] react with H_2 to form binuclear complexes of the type $(PR_3)_2H_2Rh(\mu\text{-X})_2Rh(CO)(PR_3)$ [X = Cl, Br or I, R = Ph; X = I, R = Me] and $(PMe_3)_2H(X)Rh(\mu\text{-H})(\mu\text{-X})Rh(CO)(PMe_3)$ [X = Cl, Br or I] *via* the generation and trapping of $RhH_2X(PR_3)_2$ by $RhX(CO)(PPh_3)_2$. Analogous complexes containing mixed halide bridges $(PPh_3)_2H_2Rh(\mu\text{-X})(\mu\text{-Y})Rh(CO)(PPh_3)$ [X,Y = Cl, Br or I; X ≠ Y] are detected when $RhX(CO)(PPh_3)_2$ and $RhY(CO)(PPh_3)_2$ are warmed together with p-H_2. In these reactions only one isomer of the products $(PPh_3)_2H_2Rh(\mu\text{-I})(\mu\text{-Cl})Rh(CO)(PPh_3)$ and $(PPh_3)_2H_2Rh(\mu\text{-I})(\mu\text{-Br})Rh(CO)(PPh_3)$ is formed in which the μ-iodide bridge is *trans* to the CO ligand of the rhodium(I) centre. However, when $RhCl(CO)(PPh_3)_2$ and $RhBr(CO)(PPh_3)_2$ are warmed together two isomers of $(PPh_3)_2H_2Rh(\mu\text{-Cl})(\mu\text{-Br})Rh(CO)(PPh_3)$ are produced. The results of these reactions obtained using the signal enhancements of PHIP are analysed mechanistically with a general scheme for binuclear product formation involving initial H_2 oxidative addition, facile CO loss from the resultant rhodium(III) centre, halide bridge formation with unchanged $RhX(CO)(PR_3)_2$, and subsequent formation of a second bridge along with phosphine loss. The selectivity of product formation for mixtures of the X = I and X = Cl or Br complexes leads to a deeper understanding of the mechanism of formation and the key steps of trapping the unsaturated rhodium(III) dihydride intermediate and closure of the second bridge. In view of the failure to detect readily such species under normal conditions, and bearing in mind that the largest signal enhancements reported approach 1000 fold,[1] we estimate that these products only represent between 0.01 and 1% of the species present in solution.

The $(PPh_3)_2H_2Rh(\mu\text{-X})_2Rh(CO)(PPh_3)$ products were shown to undergo hydride self exchange by EXSY spectroscopy with rates of 13.7 s^{-1} for the $(\mu\text{-Cl})_2$ complex and 2.5 s^{-1} for the $(\mu\text{-I})_2$ complex at 313 K. Activation parameters, measured by analysing the rate data as a function of temperature, indicate that ordering dominates up to the rate-determining step for the exchange; for $(\mu\text{-Cl})_2$ $\Delta H^{\ddagger} = 52 \pm 9$ kJ mol^{-1} and $\Delta S^{\ddagger} = -61 \pm 27$ J K^{-1} mol^{-1}. The exchange process proceeds *via* opening of the Rh^{III}–halide bridge which is *trans* to phosphine on the rhodium(I) centre, equilibration of hydrides, and bridge re-establishment.

When $RhX(CO)(PMe_3)_2$ [X = Cl or Br] is warmed with p-H_2

the complexes $(PMe_3)_2H(X)Rh(\mu\text{-}H)(\mu\text{-}X)Rh(CO)(PMe_3)$ [X = Cl or Br] are detected. These products contain a μ-hydride ligand which is *trans* to the rhodium(I) PMe_3 group. However, when X = I the situation is far more complex, exhibiting strong temperature dependence, with $(PMe_3)_2H_2Rh(\mu\text{-}I)_2Rh(CO)(PMe_3)$ dominating at low temperatures and $(PMe_3)_2(I)H(\mu\text{-}H)(\mu\text{-}I)Rh(CO)(PMe_3)$ predominant at higher temperatures. An additional dibridged product corresponding to a second isomer of $(PMe_3)_2(I)H(\mu\text{-}H)(\mu\text{-}I)Rh(CO)(PMe_3)$ in which the bridging hydride is *trans* to the rhodium(I) CO ligand, is also observed in this reaction. A triply bridged species, $(PMe_3)_2HRh(\mu\text{-}H)(\mu\text{-}I)_2Rh(CO)(PMe_3)$, was also observed for the iodide. Density functional calculations indicate that all four structural types correspond to minima on the potential energy surface connecting the products, with the structure containing bridging halides corresponding to the lowest energy form regardless of the identity of the halide or phosphine.

Acknowledgements

S. B. D. is grateful to the University of York (for M. G. P. and P. D. M.) and the Royal Society (field gradient unit), the EPSRC and Bruker UK (S. A. C., Case award, and spectrometer) and NATO for financial support. R. E. wishes to acknowledge financial support for this work from the National Science Foundation (Grants CHE 94–09441 and 97-29311) and NATO. A generous loan of rhodium trichloride from Johnson Matthey is acknowledged. J. E. M. acknowledges support from the University of York IRPF.

References

1 C. R. Bowers, D. H. Jones, N. D. Kurur, J. A. Labinger, M. G. Pravica and D. P. Weitekamp, *Adv. in Magn. Reson.*, 1990, **14**, 269; J. Natterer and J. Bargon, *Prog. Nucl. Magn. Reson. Spectrosc.*, 1997, **31**, 293; C. J. Sleigh and S. B. Duckett, *Prog. Nucl. Magn. Reson. Spectrosc.*, 1999, **34**, 71.
2 T. C. Eisenschmid, R. U. Kirss, P. P. Deutsch, S. I. Hommeltoft, R. Eisenberg, J. Bargon, D. G. Lawler and A. L. Balch, *J. Am. Chem. Soc.*, 1987, **109**, 8089.
3 C. R. Bowers and D. P. Weitekamp, *J. Am. Chem. Soc.*, 1987, **109**, 5541.
4 C. R. Bowers and D. P. Weitekamp, *Phys. Rev. Lett.*, 1986, **57**, 2645.
5 M. Jang, S. B. Duckett and R. Eisenberg, *Organometallics*, 1996, **15**, 2863; S. B. Duckett, R. J. Mawby and M. G. Partridge, *Chem. Commun.*, 1996, 383.
6 T. C. Eisenschmid, J. McDonald, R. Eisenberg and R. G. Lawler, *J. Am. Chem. Soc.*, 1989, **111**, 7267 J. Barkemeyer, M. Haake and J. Bargon, *J. Am. Chem. Soc.*, 1995, **117**, 2927.
7 S. B. Duckett, C. L. Newell and R. Eisenberg, *J. Am. Chem. Soc.*, 1993, **115**, 1156; M. Haake, J. Natterer and J. Bargon, *J. Am. Chem. Soc.*, 1996, **118**, 8688.
8 J. Barkemeyer, J. Bargon, H. Sengstschmid and R. Freeman, *J. Magn. Reson. Ser. A*, 1996, **120**, 129.
9 H. Sengstschmid, R. Freeman, J. Barkemeyer and J. Bargon, *J. Magn. Reson. Ser. A*, 1996, **120**, 249.
10 J. Natterer, J. Barkemeyer and J. Bargon, *J. Magn. Reson. Ser. A*, 1996, **123**, 253.
11 S. B. Duckett, G. K. Barlow, M. G. Partridge and B. A. Messerle, *J. Chem. Soc., Dalton. Trans.*, 1995, 3427; S. B. Duckett, R. J. Mawby and M. G. Partridge, *Chem. Commun.*, 1996, 383; S. P. Millar, M. Jang, R. J. Lachicotte and R. Eisenberg, *Inorg. Chim. Acta*, 1998, **270**, 363.
12 B. A. Messerle, C. J. Sleigh, M. G. Partridge and S. B. Duckett, *J. Chem. Soc., Dalton Trans.*, 1999, 1429.
13 S. Hasnip, S. B. Duckett, D. R. Taylor and M. J. Taylor, *Chem. Commun.*, 1998, 923; S. P. Millar, D. L. Zubris, J. E. Bercaw and R. Eisenberg, *J. Am. Chem. Soc.*, 1998, **120**, 5329; C. J. Sleigh, S. B. Duckett, R. J. Mawby and J. P. Lowe, *Chem. Commun.*, 1999, 1223.
14 S. B. Duckett, C. L. Newell and R. Eisenberg, *J. Am. Chem. Soc.*, 1994, **116**, 10548.
15 A. Harthun and J. Bargon, *Angew. Chem., Int. Ed. Engl.*, 1997, **109**, 1103.
16 L. Vallarino, *J. Chem. Soc.*, 1957, 2287.
17 J. A. Osborn, F. H. Jardine, J. F. Young and G. Wilkinson, *J. Chem. Soc. A*, 1966, 1711.
18 P. C. Ford, T. L. Netzel, C. T. Spillett and D. B. Poureau, *Pure Appl. Chem.*, 1990, **62**, 1091; C. T. Spillett and P. C. Ford, *J. Am. Chem. Soc.*, 1989, **111**, 1932; D. A. Wink and P. C. Ford, *J. Am. Chem. Soc.*, 1987, **109**, 436.
19 A. J. Kunin and R. Eisenberg, *Organomet.*, 1988, **7**, 2124.
20 L. Vaska and M. F. Wernke, *Trans., N. Y. Acad. Sci.*, 1971, **33**, 80.
21 S. B. Duckett and R. Eisenberg, *J. Am. Chem. Soc.*, 1993, **115**, 5292; S. B. Duckett, R. Eisenberg and A. S. Goldman, *J. Chem. Soc., Chem Commun.*, 1993, 1185; P. D. Morran, S. A. Colebrooke, S. B. Duckett, J. A. B. Lohman and R. Eisenberg, *J. Chem. Soc., Dalton Trans.*, 1998, 3363.
22 R. H. Summerville and R. Hoffmann, *J. Am. Chem. Soc.*, 1979, **101**, 3821; S. Shaik, R. Hoffmann, C. R. Fisel and R. Summerville, *J. Am. Chem. Soc.*, 1980, **102**, 4555; G. Aullón, G. Ujaque, A. Lledós, S. Alvarez and P. Alemany, *Inorg. Chem.*, 1998, **37**, 804.
23 A. Dedieu, *Inorg. Chem.*, 1980, **19**, 375; C. Daniel, N. Koga, J. Han, X. Y. Fu and K. Morokuma, *J. Am. Chem. Soc.*, 1988, **110**, 3773; N. Koga and K. Morokuma, *J. Phys. Chem*, 1990, **94**, 5454; P. Margl, T. Ziegler and P. E. Blöchl, *J. Am. Chem. Soc.*, 1995, **117**, 12625; G. P. Rosini, F. C. Liu, K. Krogh-Jesperson, A. S. Goldman, C. B. Li and S. P. Noland, *J. Am. Chem. Soc.*, 1998, **120**, 9256.
24 R. G. Parr and W. Yang, *Density Functional Theory of Atoms and Molecules*, Oxford University Press, New York, 1989.
25 G. Bodenhausen and R. R. Ernst, *J. Am. Chem. Soc.*, 1982, **104**, 1304.
26 T. Ziegler, *Chem. Rev.*, 1991, **91**, 651.
27 ADF 2.3.0, Theoretical Chemistry, Vrije Univeriteit, Amsterdam. E. J. Baerends, E. D. Ellis and P. Ros, *Chem. Phys.*, 1973, **2**, 42; G. te Velde and E. J Baerends, *J. Comput. Phys.*, 1992, **99**, 84.
28 S. H. Vosko, L. Wilk and M. Nusair, *Can. J. Phys.*, 1980, **58**, 1200.
29 A. D. Becke, *Phys. Rev. A*, 1988, **38**, 3098.
30 J. P. Perdew, *Phys. Rev. B*, 1986, **33**, 8822.
31 L. Versluis and T. Ziegler, *J. Chem. Phys.*, 1988, **88**, 322.
32 C. A. Tolman, P. Z. Meakin, D. L. Lindner and J. P. Jesson, *J. Am. Chem. Soc.*, 1974, **96**, 2762; D. W. Meek and T. J. Mazanec, *Acc. Chem. Res.*, 1981, **14**, 266.
33 C. J. Sleigh, S. B. Duckett and B. A. Messerle, *Chem. Commun.*, 1996, 2395.
34 I. J. Colquhoun and W. McFarlane, *J. Magn. Reson.*, 1982, **46**, 525.
35 K.-C. Shih and A. S. Goldman, *Organometallics*, 1993, **12**, 3390.
36 E. B. Meier, R. R. Burch and E. L. Muetterties, *J. Am. Chem. Soc.*, 1982, **104**, 2661.
37 A. J. Sivak and E. L. Muetterties, *J. Am. Chem. Soc.*, 1979, **101**, 4878.
38 H. Kessler, M. Gehrke and C. Griesinger, *Angew. Chem., Int. Ed. Engl.*, 1988, **27**, 490.
39 S. Hasnip, S. B. Duckett, D. R. Taylor, G. K. Barlow and M. J. Taylor, *Chem. Commun.*, 1999, 889.
40 B. E. Hauger, D. Gusev and K. G. Caulton, *J. Am. Chem. Soc.*, 1994, **116**, 208.

Paper 9/05109K